Giant magnetoresistance enhancement at room-temperature in organic spin valves based on $La_{0.67}Sr_{0.33}MnO_3$ electrodes

B. B. Chen, Y. Zhou, S. Wang, Y. J. Shi, H. F. Ding, and D. Wu

Citation: Appl. Phys. Lett. **103**, 072402 (2013); doi: 10.1063/1.4818614
View online: http://dx.doi.org/10.1063/1.4818614
View Table of Contents: http://aip.scitation.org/toc/apl/103/7
Published by the American Institute of Physics

RIGHTSLINK

Giant magnetoresistance enhancement at room-temperature in organic spin valves based on $La_{0.67}Sr_{0.33}MnO_3$ electrodes

B. B. Chen, Y. Zhou, S. Wang, Y. J. Shi, H. F. Ding, and D. Wu[a)]
National Laboratory of Solid State Microstructures and Department of Physics, Nanjing University, 22 Hankou Road, Nanjing 210093, People's Republic of China

(Received 11 June 2013; accepted 30 July 2013; published online 12 August 2013)

We have systematically studied the magnetoresistance (MR) of Alq_3-based organic spin valves using as-grown $La_{0.67}Sr_{0.33}MnO_3$ (LSMO), annealed LSMO, and $La_{0.67}Ca_{0.33}MnO_3$ as the bottom electrode. A giant enhancement of MR ratio (more than one order of magnitude) is observed when the optimal annealed LSMO is used, and the measured MR can be as high as 2.2% at room temperature. Below ~100 K, the temperature dependence of the normalized MR is almost identical with these three electrodes despite the strong difference in Curie temperature (from 250 K to 360 K). We attribute this similar MR temperature dependence to the spin relaxation in Alq_3.
© *2013 AIP Publishing LLC*. [http://dx.doi.org/10.1063/1.4818614]

The discovery of the giant magnetoresistance (MR) effects in the organic semiconductor (OSC) based vertical spin valve devices has initiated considerable research into the spin-dependent transport phenomena in OSCs.[1] These studies are motivated by the long spin relaxation time in OSCs, which allows the spin information to survive for very long time,[2] and the integration of the spin degree of freedom into the OSC-based electronic devices, such as organic light emitting diodes (OLEDs) and organic memory devices.[3–5] In comparison with the inorganic semiconductor devices, the organic devices promise low-cost, easy-to-fabricate, versatile organic materials and mechanical flexibility. A MR ratio as large as 300% was demonstrated at low temperature in the most-studied organic spin valve (OSV) of $La_{0.67}Sr_{0.33}MnO_3$ (LSMO)/tris(8-hyroxyquinoline) aluminum (Alq_3)/Co using a relative thick Alq_3, in which the spin-polarized carriers were injected into and transported through.[6] For practical application, it is vital to achieve large room temperature spin-dependent effects. However, the MR ratio decayed strongly with increasing temperature, and most reports showed that the MR effects vanished well below room temperature.[1,4–6] Recently, a very small MR of about 0.15% at room temperature was reported in an OSV with the device structure of LSMO/Alq_3/Al_2O_3/Co, in which the introducing of the Al_2O_3 tunnel barrier at the interface of Alq_3 and Co improved the interface and, consequently, the MR effects.[7] On the other hand, if the organic layer was thin enough to serve as a tunneling barrier, a few percent tunneling MR was observed at room temperature.[8,9] However, to fully utilize the spin degree of freedom in organic devices such as OLED, the spin-polarized carriers are required to be injected into and hop through the OSCs rather than tunnel through.

The OSVs reported to date showed that the MR effects vanished well below the Curie temperature (T_C) of two ferromagnetic electrodes.[1–7] The underlying physics for the MR temperature dependence remains a subject of debate. The similar temperature dependence of the spin diffusion length, directly measured by low energy muon spin rotation, and MR response in Alq_3-based OSVs suggested that the spin relaxation in Alq_3 layer dominated the MR temperature dependence.[10] This was further supported by a recent theoretical calculation based on the theory of spin-orbit coupling induced spin relaxation.[11] However, in the OSV of LSMO/Alq_3/Co, some experimental results showed that the MR temperature response closely resembled the surface spin polarization of LSMO film, leading to the conclusion that the ferromagnetic electrode, LSMO, was responsible for the MR temperature dependence, and the spin relaxation in Alq_3 was temperature independent.[7,12] Since the T_C of bulk LSMO was 370 K,[13] the room-temperature MR effects were expected to be better if the ferromagnetic electrodes with higher T_C were used. However, for Fe/Alq_3/Co OSV device, the MR effects disappointingly vanished around 90 K, even though the T_C of Fe and Co was above 1000 K.[14]

In this work, we systematically studied the correlation between MR effects and electrodes in Alq_3-based OSVs. We used materials with different T_C as the bottom electrode, including $La_{0.67}Ca_{0.33}MnO_3$ (LCMO) films, of which the T_C was only 250 K,[15] and LSMO films, of which the T_C can be tuned from 320 K to 360 K by annealing at different temperatures. The LSMO films showed atomically smooth surfaces with T_C comparable to the bulk LSMO after annealing at optimized conditions. The performance of OSV fabricated on optimally annealed LSMO was dramatically improved. The MR ratio was as high as 48% at low temperature and persisted to room temperature with MR ratio in excess of 2% in the typical LSMO/Alq_3/Co OSVs. Furthermore, we found that the OSVs of LSMO/Alq_3/Co and LCMO/Alq_3/Co showed very similar MR temperature dependence below ~100 K although the T_C of LCMO films was about 110 K lower than that of LSMO film, indicating that the spin relaxation in Alq_3 played an important role in MR temperature dependence.

The single crystalline ~100 nm thick LSMO films were epitaxially grown on $SrTiO_3$ (001) substrates by pulsed laser deposition (PLD) with a shadow mask to define a proper size as the bottom electrodes. The detailed information about the LSMO film growth can be found in our earlier publication.[16] The obtained LSMO films were annealed in flowing pure oxygen for 6 h at 1 atm and 900 °C, 1000 °C, 1100 °C, and 1200 °C, respectively. The surface morphologies of the

[a)]Electronic mail: dwu@nju.edu.cn

 © 2013 AIP Publishing LLC

RIGHTSLINK

annealed LSMO films were characterized by atomic force microscope (AFM) and optical microscope. The magnetic properties of LSMO films were measured by a vibrating sample magnetometer (VSM) from 300 K to 400 K and a superconducting quantum interference device VSM (SQUID-VSM) from 10 K to 300 K. The 50-nm-thick Alq_3 films were evaporated on LSMO strip at room temperature by a thermal deposition with a deposition rate of ~0.07 nm/s. Without breaking vacuum, the LSMO/Alq_3 bilayers were covered by a shadow mask and tilted to face away Co e-beam source. Then a growth method called indirect deposition was used to deposit the Co electrode.[17] This method can dramatically reduce the diffusion of top electrode into organic layer and significantly improve the OSV yield and reproducibility. The OSVs of LCMO/Alq_3/Co were fabricated in a similar process. The device area is $\sim 1 \times 1\ mm^2$. The electrical transport measurements were carried out in a four-point cross geometry with the magnetic field applied within the film plane of the electrodes.

The ferromagnetic interaction in LSMO has been recognized to be double exchange interaction between Mn^{3+} and Mn^{4+} ions through O^{2-} ions.[18] The magnetic properties of LSMO are generally believed to be greatly influenced by the oxygen content.[19] The oxygen deficiency is generally occurred in the as-grown LSMO films.[20] It is possible to anneal LSMO film to enhance the magnetization, particularly surface magnetization which is responsible for the MR effects in OSVs, to improve the performance of OSVs.

Figure 1 presents the temperature dependence of the normalized magnetization (M) (normalized to M at 10 K) with an in-plane magnetic field of 3000 Oe for the as-grown and annealed LSMO films, respectively. All these samples undergo a sharp ferromagnetic to paramagnetic transition. As expected, the T_C of all annealed LSMO increases from 320 K for as-grown sample to ~360 K, which is comparable to the T_C of bulk LSMO. This result suggests that the annealing process reduces the oxygen deficiency in the as-grown films to approach the oxygen stoichiometry of LSMO films and hence substantially improves the magnetic properties of LSMO.[21] This is also supported by the enhanced saturation magnetization after annealing, as shown in the inset of Fig. 1. Although all annealed films show almost the same T_C, the M of the LSMO film annealed at 1100 °C decays the most slowly, particularly just below T_C, than other films. This suggests that 1100 °C is the optimal annealing temperature to improve the ferromagnetic ordering in LSMO.

Since the surface morphology is important for OSV fabrication, the surface of LSMO films was examined by AFM. Figure 2 shows the steps in the morphologic evolution of LSMO films as increasing the annealing temperature. The surface of the as-grown film shows the very dense small islands [Fig. 2(a)]. The root-mean-square roughness is estimated to be 0.47 nm, and the peak-to-valley fluctuation is ~1.9 nm, indicating that the film is fairly smooth. Apparently, the film after being annealed at 1000 °C becomes smoother with the root-mean-square roughness of 0.26 nm and peak-to-valley fluctuation of ~1.3 nm [Fig. 2(b)]. The surface morphology of the film is further largely improved after being annealed at 1100 °C for 6 h. As can be seen, the surface presents very flat surface with smooth step-edges. The line profile across the step edge as marked by the black line in Fig. 2(c) is presented in Fig. 2(e). It shows that the average terrace width is ~140 nm and the average step height is

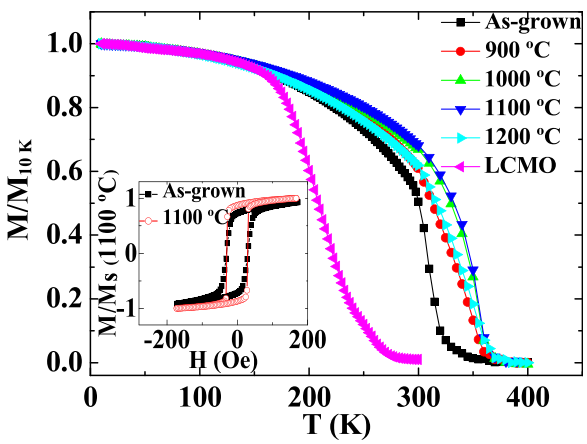

FIG. 1. Temperature dependent normalized magnetization of LSMO films annealed at different temperatures. The data are obtained with an in-plane magnetic field of 3000 Oe. For a comparison, the data of LCMO are also included. Inset: typical magnetic hysteresis loop normalized to the saturation magnetization of LSMO film annealed at 1100 °C with the field applied parallel to the film plane.

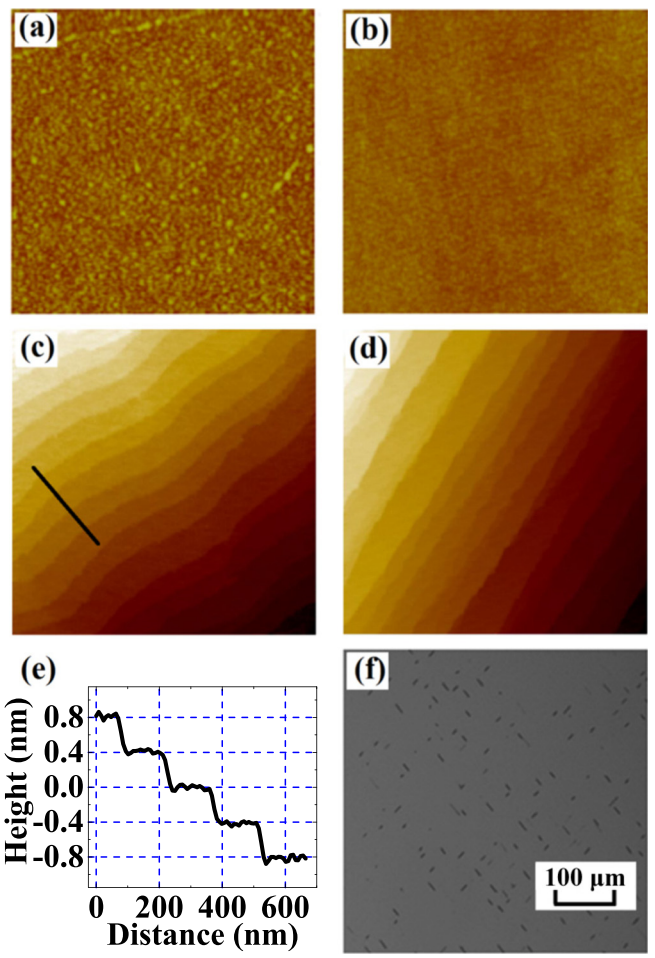

FIG. 2. (a)–(d) AFM images ($2 \times 2\ \mu m^2$) of LSMO films annealed at different temperatures: (a) as-grown, (b) annealed at 1000 °C, (c) annealed at 1100 °C, (d) annealed at 1200 °C, respectively. (e) The line profile of LSMO film as marked by the black line in (c). (f) Optical microscope image for LSMO film annealed at 1200 °C.

RIGHTSLINK

~0.4 nm, corresponding to the lattice constant of LSMO, indicating a single unit cell step-height and hence well-defined atomically flat surface formed. Annealing at higher temperature leads to step bunching, i.e., the local increase of the step density and the shrink of the terrace width [Fig. 2(d)]. Importantly, many micro-size clusters are observed on the surface under optical microscope [Fig. 2(f)]. The Sr rich surface oxide layer is observed in PLD-grown LSMO film by total reflection x-ray fluorescence.[22] These clusters might be the segregation of SrO, resulting in the off-stoichiometry of LSMO and consequently weaker ferromagnetic properties, in agreement with magnetic property measurement. Therefore, we conclude that annealing LSMO at 1100 °C for 6 h is the optimal annealing condition to reduce oxygen deficiency to enhance the ferromagnetic properties and obtain atomically smooth surface.

In the following, we will focus on studying the OSVs of LSMO (~100 nm)/Alq_3 (50 nm)/Co (25 nm) fabricated on the as-grown (device 1) and optimally annealed LSMO films (device 2). For comparison, after the measurements of device 1, the same piece of as-grown LSMO film was used to fabricate device 2 after being cleaned and annealed. The magnetic field dependence of MR is defined as $\Delta R/R_P = (R_{AP} - R_P)/R_P$, where R_P and R_{AP} correspond to the OSV resistance of two ferromagnetic electrodes in the parallel and antiparallel configurations, respectively. The results are displayed in Figs. 3(a) and 3(b), which are measured at 10 K and 2 mV. Both samples exhibit a negative MR, i.e., $R_{AP} < R_P$, consistent with previous reports with the same device structures.[1,6,12,17] Apparently, the MR ratio of device 2 is more than one order of magnitude higher than that of device 1. We note that the MR ratio is always significantly enhanced after annealing LSMO films at 1100 °C, although the MR ratio varies for OSVs fabricated on different as-grown LSMO films. The MR effect disappears below room temperature for device 1, similar to previous reports,[1,6,12,17] even though the T_C of the as-grown LSMO is still higher than room temperature. In contrast, the MR effect persists up to room temperature with MR ratio as high as 2.2% for device 2, as shown in Fig. 3(c), indicating the possibility of the applications in the field of the organic spintronics. This represents a sizeable improvement with respect to the previous results obtained from the similar OSV structures.[1,5–7,12,17] The surface roughness of Alq_3 film grown on both types of LSMO is similar (not shown here), regardless of the difference of the LSMO morphology [Figs. 2(a) and 2(c)]. The top Co/Alq_3 interfaces are essentially the same for both samples. Comparing our results using atomically-flat LSMO with previous study using non-atomically-flat LSMO,[23] we find that the MR ratio is not influenced by the LSMO roughness. The theoretical calculations and photoemission studies show that the spin polarization of the LSMO surface is sensitive to the oxygen vacancy.[24] Since the as-grown LSMO is usually oxygen deficient, we attribute the increase of MR ratio to the enhancement of surface spin polarization of LSMO after the annealing.

Figure 4(a) shows the normalized MR ratio as a function of temperature for devices 1 and 2, which monotonically decreases with increasing temperature. The MR temperature response is possibly related to the temperature dependences of these three factors: (i) the spin injection efficiency at ferromagnetic/organic interfaces, (ii) the surface spin polarization of ferromagnetic electrodes, and (iii) the spin relaxation in Alq_3. The former two mechanisms can be excluded by the following arguments. First, in our previous study, we find that the spin injection efficiency relies on the interfacial barrier height.[25] The interfacial barrier height is the difference between the Fermi level of the electrodes and the highest occupied or lowest unoccupied molecular orbital levels of the organic layer, which are weakly temperature dependent. Meanwhile, we find that the MR temperature dependence is

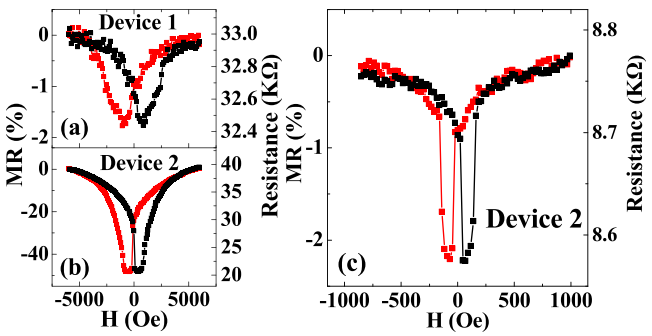

FIG. 3. MR curves of OSV devices fabricated on (a) as-grown LSMO film, (b) optimally annealed LSMO film, respectively, at 10 K. (c) Room temperature MR curve for OSV fabricated on optimally annealed LSMO film.

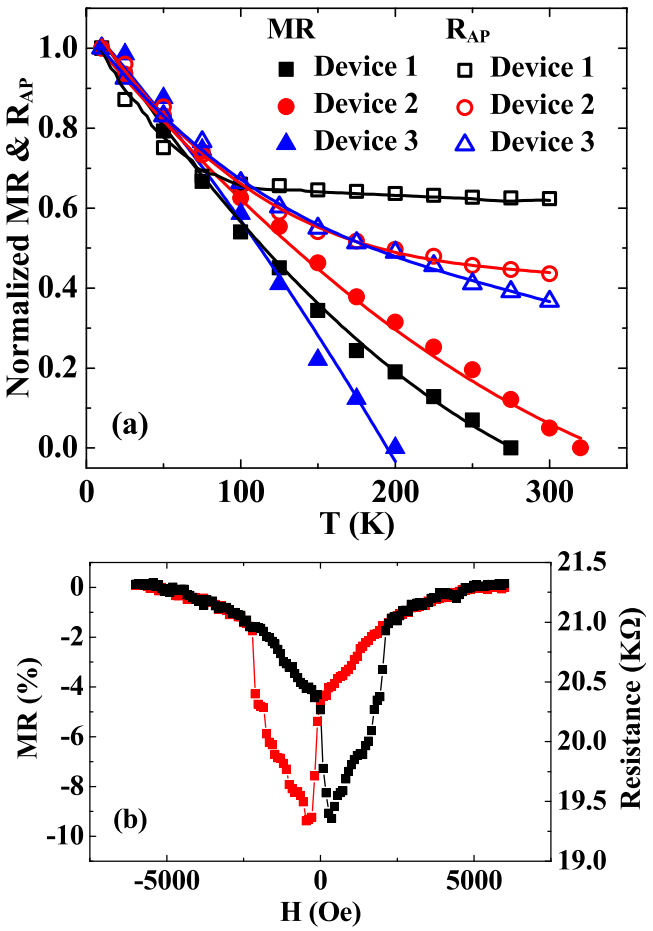

FIG. 4. (a) The normalized temperature dependence of MR and resistance in the antiparallel magnetic configuration of devices 1, 2, and 3, respectively. The lines are guided to the eyes. (b) Typical MR curve of OSV device fabricated on LCMO film measured at 100 K.

RIGHTSLINK

not altered by the spin injection efficiency.[25] Thus the MR temperature dependence is improbably originated from the spin injection efficiency. Second, the as-grown LSMO films show lower T_C, inferring that the spin polarization of the as-grown LSMO films and the corresponding MR temperature dependence decrease more rapidly with increasing temperature than that of the annealed LSMO films. However, the MR ratio decreases in almost the same rate below ~100 K regardless of the distinct difference of MR ratio for devices 1 and 2. The disagreement between the experimental observation and the expectation indicates that the spin polarization of LSMO alone cannot explain the MR temperature dependence. As discussed, the spin injection efficiency and LSMO spin polarization should not be the origin of the MR temperature dependence below ~100 K. The spin relaxation in Alq_3 is the only main reason for MR temperature dependence, indicating that the spin relaxation in Alq_3 is temperature dependent, and it has the same temperature response as MR below ~100 K.

To further strengthen the above arguments, we fabricated the OSVs of LCMO (100 nm)/Alq_3 (50 nm)/Co (25 nm) (device 3). As shown in Fig. 4(b), the device 3 exhibits MR of 9% at 100 K and 10 mV. In this device the only difference from devices 1 and 2 is that the bottom electrode is LCMO. From Fig. 1, it can be clearly seen that the T_C of LCMO is about 250 K, which is 110 K lower than that of LSMO. The spin polarization of LCMO film should decrease much more rapidly with temperature than that of LSMO due to lower T_C.[26] If the spin polarization of LCMO has impact on MR, the MR of device 3 would decrease more rapidly with temperature than that of devices 1 and 2. However, this clearly is not the case below ~100 K [Fig. 4(a)], supporting our extrapolation that the spin relaxation in Alq_3 dominates the temperature dependence in this temperature range. In addition, Fig. 4(a) clearly shows that the MR ratio and R_{AP} versus temperature for these three different devices follow the same trend below ~100 K, indicating the correlation between MR and resistance. This feature also strongly supports that the spin is relaxed during the transport through Alq_3 layer.[27,28] Moreover, our arguments is also supported by a recent theoretical calculation and an experiment that the spin diffusion length in Alq_3 strongly is dependent on temperature below about 80–100 K and levels off above 80–100 K.[10,11,29] Above ~100 K, since the spin diffusion length is almost constant with increasing temperature, the spin polarization of the electrodes (LCMO or LSMO) starts to play a role, resulting that the MR ratio of device 3 decreases the most rapidly than the other devices.

In summary, we have shown that a room temperature MR of 2.2% in typical OSV of LSMO/Alq_3/Co with 50-nm-thick Alq_3 is observed after the LSMO electrode is annealed at 1100 °C for 6 h. This achievement is attributed to the enhanced surface spin polarization of the LSMO films by reducing the oxygen vacancies through annealing. The annealed LSMO films show the increase of Curie temperature and the atomically flat surface. The MR temperature dependence shows similar trend below ~100 K for OSV fabricated on LSMO and LCMO despite the remarkably different T_C of the electrodes, suggesting that the spin relaxation in Alq_3 dominates the MR temperature response below ~100 K.

This work was supported by National Basic Research Program of China (2010CB923402 and 2013CB922103), NSF of China (11222435, 10974084, and 11023002), the Priority Academic Program Development of Jiangsu Higher Education Institutions, and the Fundamental Research Funds for the Central Universities.

[1]Z. H. Xiong, D. Wu, Z. V. Vardeny, and J. Shi, Nature (London) **427**, 821 (2004).
[2]G. Szulczewski, S. Sanvito, and M. Coey, Nature Mater. **8**, 693 (2009).
[3]V. A. Dediu, L. E. Hueso, I. Bergenti, and C. Taliani, Nature Mater. **8**, 707 (2009).
[4]T. D. Nguyen, E. Ehrenfreund, and Z. V. Vardeny, Science **337**, 204 (2012).
[5]M. Prezioso, A. Riminucci, I. Bergenti, P. Graziosi, D. Brunel, and V. A. Dediu, Adv. Mater. **23**, 1371 (2011).
[6]D. Sun, L. Yin, C. Sun, H. Guo, Z. Gai, X.-G. Zhang, T. Z. Ward, Z. Cheng, and J. Shen, Phys. Rev. Lett. **104**, 236602 (2010).
[7]V. Dediu, L. E. Hueso, I. Bergenti, A. Riminucci, F. Borgatti, P. Graziosi, C. Newby, F. Casoli, M. P. De Jong, C. Taliani, and Y. Zhan, Phys. Rev. B **78**, 115203 (2008).
[8]K. Li, Y. Chang, S. Agilan, J. Hong, J. Tai, W. Chiang, K. Fukutani, P. A. Dowben, and M. Lin, Phys. Rev. B **83**, 172404 (2011).
[9]T. S. Santos, J. S. Lee, P. Migdal, I. C. Lekshmi, B. Satpati, and J. S. Moodera, Phys. Rev. Lett. **98**, 016601 (2007).
[10]A. J. Drew, J. Hoppler, L. Schulz, F. L. Pratt, P. Desai, P. Shakya, T. Kreouzis, W. P. Gillin, A. Suter, N. A. Morley, V. K. Malik, A. Dubroka, K. W. Kim, H. Bouyanfif, F. Bourqui, C. Bernhard, R. Scheuermann, G. J. Nieuwenhuys, T. Prokscha, and E. Morenzoni, Nature Mater. **8**, 109 (2009).
[11]Z. G. Yu, Phys. Rev. Lett. **106**, 106602 (2011).
[12]F. J. Wang, C. G. Yang, Z. V. Vardeny, and X. G. Li, Phys. Rev. B **75**, 245324 (2007).
[13]A. Urushibara, Y. Moritomo, T. Arima, A. Asamitsu, G. Kido, and Y. Tokura, Phys. Rev. B **51**, 14103 (1995).
[14]F. J. Wang, Z. H. Xiong, D. Wu, J. Shi, and Z. V. Vardeny, Synth. Met. **155**, 172 (2005).
[15]J. W. Lynn, R. W. Erwin, J. A. Borchers, Q. Huang, A. Santoro, J.-L. Peng, and Z. Y. Li, Phys. Rev. Lett. **76**, 4046 (1996).
[16]Y. J. Shi, Y. Zhou, H. F. Ding, F. M. Zhang, L. Pi, Y. H. Zhang, and D. Wu, Appl. Phys. Lett. **101**, 122409 (2012).
[17]S. Wang, Y. J. Shi, L. Lin, B. B. Chen, F. J. Yue, J. Du, H. F. Ding, F. M. Zhang, and D. Wu, Synth. Met. **161**, 1738 (2011).
[18]C. Zener, Phys. Rev. **82**, 403 (1951).
[19]J. Dho, N. H. Hur, I. S. Kim, and Y. K. Park, J. Appl. Phys. **94**, 7670 (2003).
[20]T. Li, B. Wang, H. Dai, Y. Du, and H. Yan, J. Appl. Phys. **98**, 123505 (2005).
[21]S. H. Seo, H. C. Kang, H. W. Jang, and D. Y. Noh, Phys. Rev. B **71**, 012412 (2005).
[22]T. T. Fister, D. D. Fong, J. A. Eastman, P. M. Baldo, M. J. Highland, P. H. Fuoss, K. R. Balasubramaniam, J. C. Meador, and P. A. Salvador, Appl. Phys. Lett. **93**, 151904 (2008).
[23]W. Xu, G. J. Szulczewski, P. LeClair, I. Navarrete, R. Schad, G. Miao, H. Guo, and A. Gupta, Appl. Phys. Lett. **90**, 072506 (2007).
[24]S. Picozzi, C. Ma, Z. Yang, R. Bertacco, M. Cantoni, A. Cattoni, D. Petti, S. Brivio, and F. Ciccacci, Phys. Rev. B **75**, 094418 (2007).
[25]F. J. Yue, Y. J. Shi, B. B. Chen, H. F. Ding, F. M. Zhang, and D. Wu, Appl. Phys. Lett. **101**, 022416 (2012).
[26]V. S. Amaral, J. P. Araujo, A. A. C. S. Lourenco, P. B. Tavares, Y. G. Pogorelov, J. B. Sousa, and J. M. Vieira, J. Magn. Magn. Mater. **226**, 942 (2001).
[27]C. Barraud, P. Seneor, R. Mattana, S. Fusil, K. Bouzehouane, C. Deranlot, P. Graziosi, L. Hueso, I. Bergenti, V. Dediu, F. Petroff, and A. Fert, Nat. Phys. **6**, 615 (2010).
[28]Y. Lu, M. Tran, H. Jaffrès, P. Seneor, C. Deranlot, F. Petroff, J.-M. George, B. Lépine, S. Ababou, and G. Jézéquel, Phys. Rev. Lett. **102**, 176801 (2009).
[29]Z. G. Yu, Phys. Rev. B **85**, 115201 (2012).

RIGHTSLINK